Journal of Thermal Analysis and Calorimetry (2018) 134:181–187
https://doi.org/10.1007/s10973-018-7527-x

Crystallisation kinetics and structure of modified Zn–Al–Cu alloys

M. Krupiński[1]

Received: 6 April 2018 / Accepted: 3 July 2018 / Published online: 13 July 2018

Abstract
The primary purpose of the work was to try to answer the following questions: How will the addition of lanthanum and cerium affect the crystallisation kinetics of the alloys tested? What will be the relationship between changes in the shape of the derivative curve and the microstructure and the same properties of Zn–Al10–Cu1 alloys? To improve properties of the casting zinc alloy, modification of the structure consisting in the change in the morphology of alloy structural constituents has been applied, primarily by reducing interfacial eutectic $\alpha' + \eta$, reduction in the size of fundamental components, as well as the effect of La on the change in the grain morphology of the solid solution with the aluminium matrix from the dendritic one to the "tweed" one. To describe the phenomena that occur in the material during solidification as a result of the application of modifiers, the thermal derivative analysis and structural analysis using scanning and transmission electron microscopy method were carried out.

Keywords Casting alloys · Crystallisation kinetics · Zn–Al alloy · La modification

Introduction

The functional properties of cast zinc alloys depend on the primary structure of the alloy, which is dependent on the crystallisation kinetics [1–4]. The crystallisation kinetics are determined by the following parameters: temperature of the liquid metal, cooling rate, generation of latent heat of crystallisation, density and distribution of formed nuclei, fraction solid, concentration of components in the remaining liquid metal, values describing the structure at this distance, and quantities defining the shape and size of structural elements. All these parameters may vary depending on the time of crystallisation and geometrical parameters of the cast. Temperature changes, cooling rates, and the fraction solid are determined experimentally using thermal analysis or thermal derivative analysis. The full characterisation of the crystallisation kinetics can be obtained by combining the crystallisation with the heat exchange equations [5–7].

✉ M. Krupiński
mariusz.krupinski@polsl.pl

[1] Institute of Engineering Materials and Biomaterials, Silesian University of Technology, Konarskiego St. 18a, 44-100 Gliwice, Poland

The Zn–Al alloys with a high amount of Al elements require a melting temperature about 700–750 °C, which can cause oxidation of the alloy, increasing energy costs. The application of ZnTi4 modifiers has a good solubility at much lower temperatures, i.e. about 500 °C, thus avoiding harmful overheating and allowing to save energy costs. The application of ZnTi modifiers serves as a substrate for nucleation of intermetallic Al_3Ti phases for the heterogeneous nucleation of the α' phase [8, 9].

The literature presents the results of the application of rare earth (RE) elements on the structure and properties of alloys to modify the microstructure. In the paper [10], it was found that the addition of RE elements makes it difficult the diffusion of atoms, causes a reduction in the phenomenon of combining particles as a result of coagulation. This prevents the coalescence of particles ensuring homogeneity of the microstructure.

Low concentration of lanthanum in the alloy results in the formation of a "reticulated" structure, which increases the corrosion resistance, while too high lanthanum above 1% by mass reduces the amount of Al in the matrix, which increases the corrosion rate. In aluminium alloys, the addition of lanthanum results in the nucleation of the two-component $Al_{11}La_3$ phase along the grain boundaries and at their borders, which is an effective barrier to dislocation movement near the grain boundaries [11, 12].

The results presented in [13] show that a small amount of Ce and La added to Zn alloys improves its resistance to corrosion. In the zinc alloys, RE elements are homogeneously dispersed formed by precipitation in the zinc matrix—the phase of the intermetallic compounds CeZn11 and LaZn13—following generally known phase equilibrium systems. In the case of Zn–Ce–La alloys (composition of mischmetal), intermetallic compounds have been characterised as Ce1−xLaxZn11 and CeyLa1−yZn13.

Methodology and material

One of the primary issues was to create research programme so that it would be possible to determine the effect of the modifier concentration, on the structure. The effectiveness of the modification was described by the degree of refinement of the microstructure components, as well as changes in the features of the modified alloys, as well as by the analysis of cooling curves of the tested alloys. To describe the phenomena that occur in the material during solidification under various conditions caused by the applied modifiers that provide the basis for heterogeneous nucleation, it was decided to use thermal derivative analysis methods. The mentioned method allows to accurately describe and interpret the crystallisation kinetics of the tested materials. This methodology allows determining the relationship between the crystallisation kinetics and the set of functional properties of cast zinc alloys with the addition of aluminium and copper, both unmodified and modified with La and Ce.

In particular, the scope of the tests carried out included the following issues:

- Thermal derivative analysis (TDA) using a UMSA metallurgical simulator of tested alloys cooled freely, primarily to determine the nucleation temperature (T_L) and end solidus temperature (T_{Sol}) and phase transitions in both alloys, i.e. before and after modification.
- Microstructure analysis of Zn–Al–Cu alloys, using light microscopy methods, stereological studies, and scanning electron microscopy.
- The application of image analysis methods to calculate the percentage of intermetallic phases, and to determine the changes in their morphology depending on the degree of modification.
- Chemical and phase composition analysis, identification of intermetallic phases, including their influence on the strength properties, hardness, and elastic properties, combined with structural analysis using scanning and transmission electron microscopy, and WDS X-ray microanalysis, as well as diffraction methods.

The alloys were prepared in a resistance furnace in chamotte-graphite crucibles. Alloys with additions of La and Ce were made using an argon protective atmosphere during melting. The temperature of the liquid alloy did not exceed 750 °C, and the alloy additions were added in the form of pure elements. The prepared composites were cast into a metal–carbon steel mould. Control tests of mass concentrations of Al, Cu, La, and mischmetal alloy additions were made following the OES ICP test procedure on the ULTIMA 2 Jobin–YVON device. The chemical composition of the obtained alloys is given in Table 1.

The thermal analysis of the tested alloys was carried out on the UMSA MT5 device. The heating scheme is shown in Fig. 1. From the prepared experimental melts, samples for thermal tests of ø30 × 35 mm were prepared, which were then melted in a graphite crucible. Thermocouples, in all of the experiments, were placed in the same place (heat node). For samples that were freely cooled down, the value of the cooling rate was approx. 0.1 °C s^{-1}. The cooling rate (CR) was calculated based on equation: $CR = (T_L - T_{Sol})/(t_{Sol} - t_L)$.

The thermal capacity was calculated as the sum of the mass products of the concentration of the alloy components and their specific heat.

Samples for tests were cut in a plane passing through the centre of the ingot. The prepared samples etched in reagent: 10% HF (T-HF). The etching time and reagent concentration were selected experimentally for each tested alloy. Metallographic examinations were performed using metallgraphic microscopes Leica MEF4A, Zeiss Axio Observer, Olympus LEXT OLS4000, using a computer

Table 1 Chemical composition of analysed Zn alloys

Determination of the alloy	Mass concentration of alloying elements in tested alloys/%			
	Al	Cu	La	Ce
ZnAl	10.02	0.98	–	–
ZnAl(0.3La)	10.07	1.09	0.29	–
ZnAl(0.1MM)	11.27	0.96	0.084	0.031

The designations in brackets specify the mass % of the content of individual elements or the sum of these elements

MM mischmetal

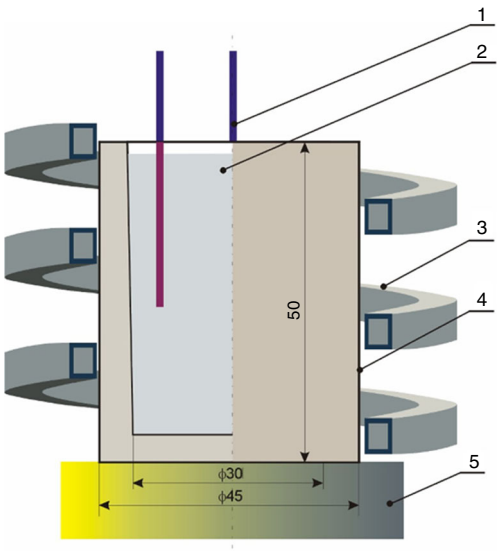

Fig. 1 Scheme of the heating system of UMSA device: 1—thermocouple, 2—sample, 3—heating coil, 4—graphite mould, 5—ceramic isolator

image analysis system at magnifications from 50 to 500 times.

Analysis of the microstructure of thin foils and phase identification of the precipitates were made utilising transmission electron microscope (TEM) JEOL 3010CX, at an accelerating voltage of 300 kV using electron diffraction to identify phase components.

Results discussion

A representative cooling curve of the Zn–Al alloy cooled down with 0.1 °C s^{-1} in the temperature range from 460 to 350 °C is shown in Fig. 2. Analysis of crystallisation process based on cooling and first derivative curves it was found that at the T_L the nucleation process of the α-phase begins, which is illustrated on the first derivative in the form of a slight inflection at a point *I* and a temporary decrease in the cooling rate of the alloy. Although the thermal effects accompanying the nucleation process and growth of α-crystals provide additional heat to the forming mixture of liquid and solid phase, the thermal balance of the cooling ingot is negative. The chemical composition of the remaining liquid changes according to the liquidus line of the Zn–Al binary system. In this range, approx a constant negative value of the first derivative is observed. The liquid enriches itself more and more in the Zn, and when the temperature $T_{(Al+Zn)}$ is reached, nucleation of the eutectic (α + η) occurs (point II). As a result of further cooling, the remaining liquid crystallises theoretically at a constant temperature $T_{E(Al+Zn)}$ ($dT/dt = 0$) to create the eutectic α + η. The crystallisation process ends when the alloy reaches the T_{Sol} temperature. In practice, the temperature for the beginning and end of the eutectic transformation shows little difference, so it was assumed that the temperature of solidus T_{Sol} is the point corresponding to point III (end of eutectic nucleation).

As a result of the thermodynamic parameters analysis of the ZnAl alloy, the appropriate values of specific heat in a

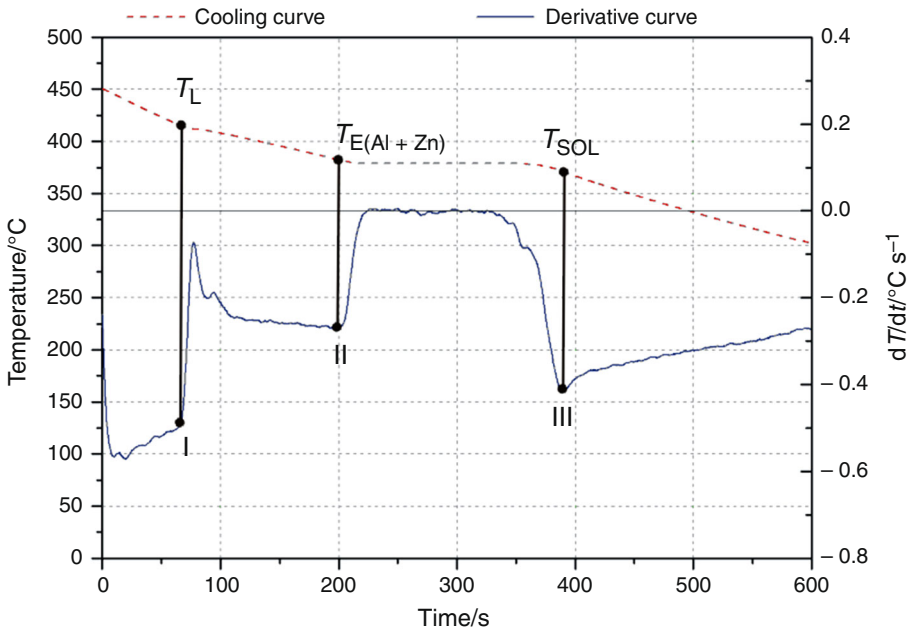

Fig. 2 Cooling and derivative curves of ZnAl alloy, cooling rate 0.1 °C s^{-1}

Table 2 Latent heat of the components and their percentage in the general latent heat of the ZnAl alloy cooled down with 0.1 °C s^{-1}

Heat capacity in liquid state Cp_l/J g^{-1} °C^{-1}	Heat capacity in solid state Cp_s/J g^{-1} °C^{-1}		Mass of sample/g
0.5305	0.4407		152.08
Reaction	Latent heat of crystallisation		Percentage/%
	Samples/J	Unit mass of a sample/J g^{-1}	
L → α	576.73	3.79	7.63
L → $E_{(\alpha+\eta)}$	6723.56	44.21	92.37
Total	7300.29	48.00	100

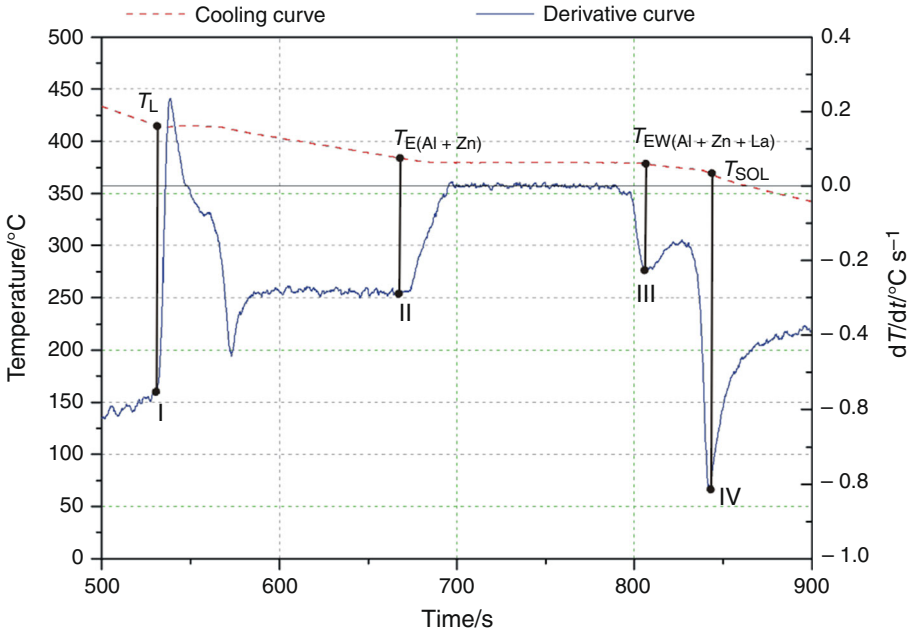

Fig. 3 Cooling and derivative curve of the ZnAl(0.3La) alloy cooled down with 0.1 °C s^{-1}

Table 3 Latent heat of the components and their percentage in all latent heat of the ZnAl(0.3La) alloy cooled down with 0.1 °C s^{-1}

Heat capacity in liquid state Cp_l/J g^{-1} °C^{-1}	Heat capacity in solid state Cp_s/J g^{-1} °C^{-1}		Mass of sample/g
0.528	0.44		148.14
Reaction	Latent heat of crystallisation		Percentage/%
	Samples/J	Unit mass of a sample/J g^{-1}	
L → α	433.78	2.93	5.07
L → E(α + η)	6841.56	46.18	86.71
L → α + η + La	592.33	3.40	8.22
Total	7867.67	52.51	100

liquid state (C_{pl}) and solid state (C_{ps}) were determined, which are presented in Table 2. The calculations of the latent heat of crystallisation of the components of analysed alloys and their percentage were presented.

In alloys with the La addition, in the crystallisation process characteristic thermal changes can be determined, indicating the formation of La-rich multi-component eutectic (Fig. 3, point III), which crystallisation begins at $T_{EW(Al+Zn+La)}$ and keep on until the T_{Sol} temperature is reached (point IV, Fig. 3). Modification of the Zn–Al–Cu alloy with La causes rise temperature the nucleation point of the α + $\eta_{(Al+Zn)}$ eutectic and decrease the temperature (T_{Sol}) of the alloy.

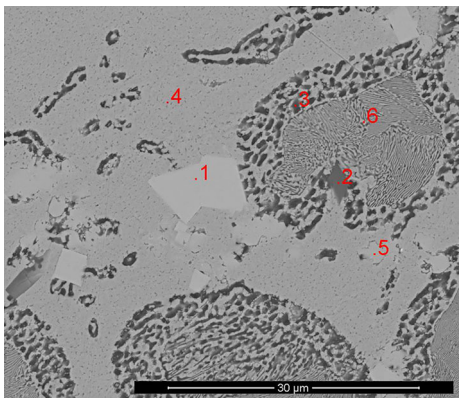

Fig. 4 Microstructure of ZnAl alloy after modification by La, cooled down with 0.1 °C s^{-1}

Table 4 Results of the quantitative WDS analysis of the chemical composition of the ZnAl(1La) alloy cooled at the rate of 0.1 °C s^{-1} made at the places marked in Fig. 4

Marking the analysis point	Mass concentration of the element/%				
	Al	La	Cu	Zn	O
1	3.40	29.42	3.60	63.59	–
2	64.40	–	1.78	10.39	–
3	54.76	–	–	40.42	4.82
4	2.88	–	–	97.12	–
5	10.69	31.53	2.90	54.88	–
6	24.63	–	–	75.37	–

Table 3 shows the calculated values of specific heat in the liquid state C_{pl} and solid state C_{ps}, a latent heat of the components of the tested alloys, and their percentage.

As the qualitative analysis requires the supplementation of information about the percentage of elements in structural components, the SEM image of the same sample was added again (Fig. 4) by providing in Table 4 the results of the chemical analysis carried out by WDS at the locations indicated in the figure.

In addition to analyses of the structure of the components of the tested alloys, transmission electron microscopy tests were carried out, which, among others, confirmed the occurrence of Zn_5La precipitates in the matrix of modified ZnAl(0.3La) alloy (Fig. 5). Application of the diffraction analysis, the Zn (η) phase with hexagonal lattice assigned to the P63/MMC space group with parameters $a = b = 0.2748$ nm and $c = 0.5167$ nm, which are the values slightly larger compared to the theoretical value for pure zinc ($a = 0.266$ nm, $c = 0.494$ nm). Also, Zn_5La grains with 0.5 µm have been confirmed in the Zn matrix.

In the modified alloys by Ce and La, determining the characteristic thermal changes during crystallisation

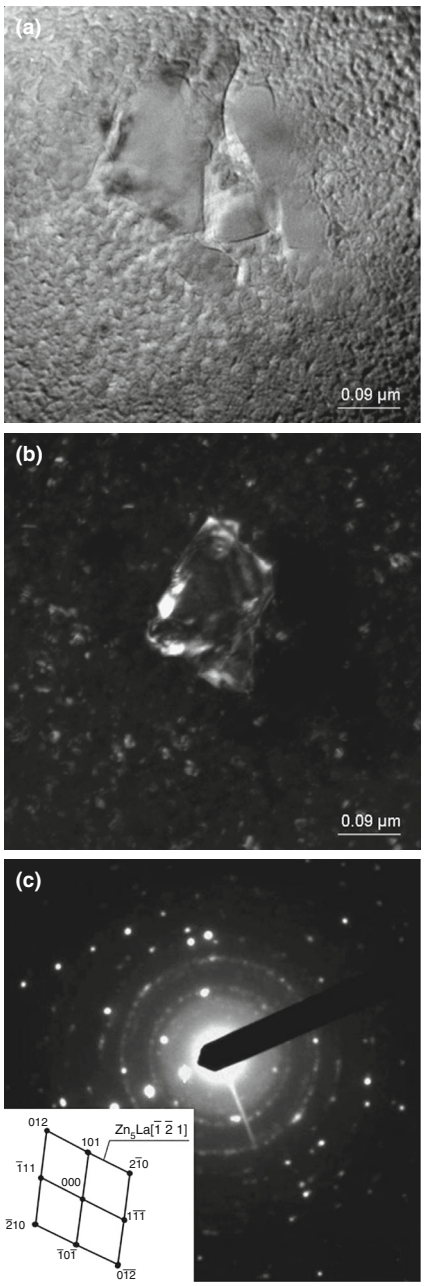

Fig. 5 Structure of the ZnAl(0.3La) alloy cooled down with 0.1 °C s^{-1}: **a** bright field; **b** dark field from (101) area; **c** diffraction pattern from 5a area with $Zn_5La\ [\bar{1}\ \ \bar{2}\ \ 1]$

process indicates the lack of formation of Ce or La-rich multi-component eutectics. The crystallisation process starts with the nucleation of the α phase (point I, Fig. 6), followed by the α + η eutectic (a point II, Fig. 6) and keeps on until the T_{Sol} temperature is reached (point III, Fig. 6).

Table 5 presents the values of the specific heat in the liquid state C_{pl} and solid state C_{ps} for the alloy with La and Ce. The calculated latent heat of crystallisation of the

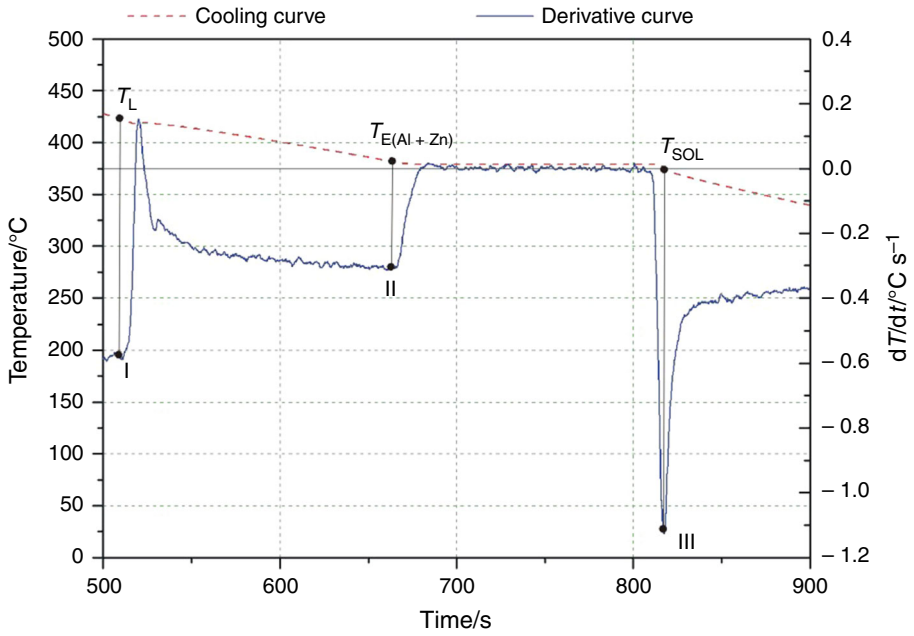

Fig. 6 Cooling and crystallisation curve of the ZnAl(0.1MM) alloy cooled down with 0.1 °C s^{-1}

Table 5 Latent heat of the components and their percentage in the general latent heat of the ZnAl(0.1MM) alloy cooled down with 0.1 °C s^{-1}

Heat capacity in liquid state Cp_l/ J g^{-1} °C^{-1}	Heat capacity in solid state Cp_s/ J g^{-1} °C^{-1}		Mass of sample/g
0.5289	0.441		150.71
Reaction	Latent heat of crystallisation		Percentage/%
	Samples/J	Samples/J	
L → α	551.15	3.66	6.65
L → $E_{(\alpha+\eta)}$	7093.56	47.07	93.35
Total	7644.71	50.73	100

components of the tested alloys as well as their percentage was also included.

Metallographic analysis using light and electron microscopy gives possibilities to characterise the morphology and chemical composition of precipitates occurring in the structure of Zn–Al–Cu alloys with the La addition, with an even diagonal system of α precipitates, sometimes called the "tweed" structure (Fig. 7b), in comparison with the Zn–Al–Cu alloy without modification (Fig. 7a) and modification by mischmetal (Fig. 7c).

Summary

The structural analyses carried out confirm the directionality of the α phase crystallisation and its uniform distribution in the material. Besides, due to the modification with La, fragmentation of precipitates can be observed, which was also confirmed by the image analysis. They also have a reduced range between the minimum and maximum value of the field and perimeter of the structural components, which indicates a more homogeneous structure.

Observations of microstructure carried out with scanning electron microscope and X-ray quantitative microanalysis confirm the presence of $\alpha' + \eta$ eutectic components, copper zinc solution in the zinc matrix, and Zn_5La precipitates with irregular shapes with sharp edges, which in most cases crystallise inside eutectics regions.

The structural tests show that the Zn–Al–Cu alloy is characterised by a typical microstructure formed during crystallisation process in which a solid solution of aluminium (α) grains in zinc solution and $\alpha + \eta$ eutectic occur, where α' phase is formed as a result eutectoidal transformation ($\alpha \rightarrow \alpha'$).

The modification of the zinc alloy with La causes formation, apart from the aluminium precipitates (α' solution), and eutectic $\alpha' + \eta$, the Zn_5La phase, which are part of the multi-component eutectic. Modification with La and Ce [14] causes the microstructure to take a "tweed" form.

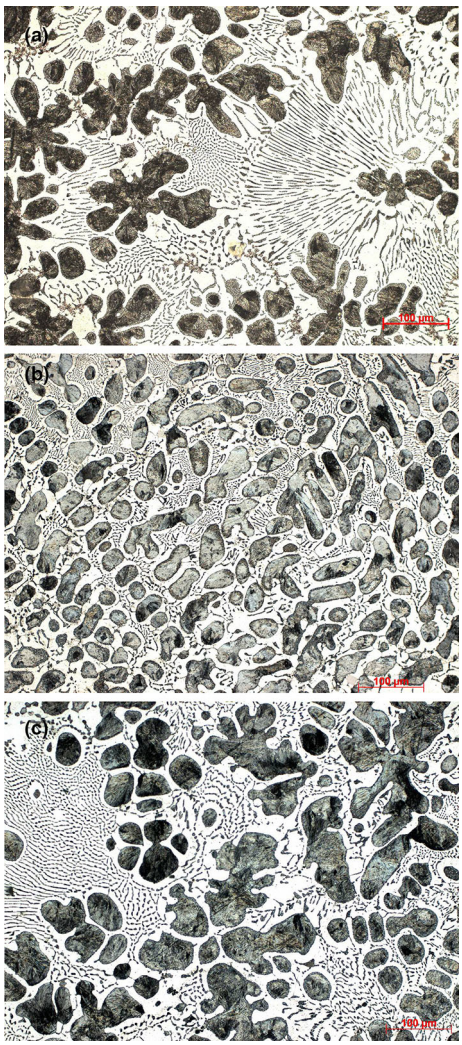

Fig. 7 Structure of the alloy; cooling rate 0.1°C s^{-1}: **a** ZnAl, T-HF; #1 $-\alpha'$ and η "small eutectics"; # $2-\alpha'+\eta$ eutectic, **b** ZnAl(0.3La), T-HF, **c** ZnAl(0.1MM), T-HF

Using both the La and Ce modifiers, no such dependencies were noticed. The addition of lanthanum reduces the nucleation temperature of the α-phase and the end temperature of crystallisation of tested alloy.

In the modified Zn–Al–Cu alloys, morphology structural components are changed, which is indicated by a reduction in the distance of the dendrite arms. The modification of the Zn–Al–Cu alloy with the addition of La causes a change in the morphology of Al precipitates from dendritic to "tweed" form, which makes it impossible to precisely measure the distance of the dendrite arms and compare the results before and after the modification. However, based on the analysis of the structure, it was found that the modification of La causes fragmentation of the structural components.

Acknowledgements This publication was financed by the Ministry of Science and Higher Education of Poland as the statutory financial grant of the Faculty of Mechanical Engineering SUT.

References

1. Krupinski M, Labisz K, Tanski T, Krupinska B, Krol M, Polok-Rubiniec M. Influence of Mg addition on crystallisation kinetics and structure of the Zn–Al–Cu alloy. Arch Metal Mater. 2016;61(2):785–9.
2. Andberg L, Bäckerud L, Chai G, Tamminen J. Solidification characteristics of aluminum alloys. 3rd ed. Illinois: AFS; 1996.
3. Krupinski M, Krupinska B, Labisz K, Rdzawski Z, Tanski T. Effect of chemical composition modification on structure and properties of the cast Zn–Al–Cu alloys. Proc Inst Mech Eng Part L: J Mater Des Appl. 2016;230(3):805–12.
4. Król M. Effect of grain refinements on the microstructure and thermal behaviour of Mg–Li–Al Alloy. J Therm Anal Calorim. 2018. https://doi.org/10.1007/s10973-018-7223-x.
5. Król M, Tański T, Sitek W. Thermal analysis and microstructural characterization of Mg–Al–Zn system alloys. Mater Sci Eng. 2015;95:012006.
6. Fras E, Kapturkiewicz W, Burbelko A, Lopez HF. A new concept in thermal analysis of castings. AFS Trans. 1993;101:505–11.
7. Kierkus WT, Sokolowski JH. Recent advances in cooling curve analysis: a new method for determining the 'Base Line' equation. AFS Trans 1999;107.
8. Krajewski WK, Zak PL, Orava J, Greer AL, Krajewski PK. Structural stability of the high-aluminium zinc alloys modified with Ti addition. Arch Foundry Eng 2012;12(1):61–66.
9. Krajewski WK. Structure and properties of high-aluminium zinc alloys inoculated with Ti addition. Arch Found. 2005;5:231–40.
10. Chen TJ, Hao Y, Sun J, Lia YD. Effects of Mg and RE additions on the semi-solid microstructure of a zinc alloy ZA27. Sci Techol Adv Mater. 2003;4:495–502.
11. Fan Y, Wu G, Gao H, Li G, Zhai C. Influence of lanthanum on the microstructure, mechanical property and corrosion resistance of magnesium alloy. J Mater Sci. 2006;41:5409–16.
12. Anyanwu IA, Gokan Y, Suzuki A, Kamado S, Kojima Y, Takeda S, Ishida T. Effect of substituting cerium-rich mischmetal with lanthanum on high temperature properties of die-cast Mg–Zn–Al–Ca–RE alloys. Mater Sci Eng A. 2004;380:93–9.
13. Veys-Renaux D, Guessoum K, Rocca E, David N, Belhamel K. New zinc–rare earth alloys: influence of intermetallic compounds on the corrosion resistance. Corrosion Sci. 2013;77:342–9.
14. Krupiński M, Krupińska B, Rdzawski Z, Labisz K, Tański T. Additives and thermal treatment influence on microstructure of nonferrous alloys. J Therm Anal Calorim. 2015;120(3):1573–83.